

Figure 3. Spectra obtained with the spectral-solubility method for a solution of CHA (at molar concentration 2.29×10^{-3}) in carbon tetrachloride at constant iodine activity at 25° ; curve A represents the system $\text{TMAI}_2\text{-TMAI}_3\text{-CCl}_4$ (uncomplexed iodine concentration of $5.30 \times 10^{-4} M$), curve B the corresponding system with CHA added to the carbon tetrachloride, and curve C the difference between curves A and B; spectra correspond to a cell path length of 1 cm.

shifted iodine band should increase with increasing stability of the complex through a series of similar donors. Figure 3 shows the visible spectra obtained with the spectral solubility method.

The charge-transfer band of $\text{CHA} \cdot \text{I}_2$ in heptane has a maximum at about 244 nm where the absorptivity is approximately $29,800 \text{ l. mol}^{-1} \text{ cm}^{-1}$. It is estimated

that $\Delta\nu_{1/2}$ of the band is 6320 cm^{-1} , and from eq 4 and 5, f and μ_{mn} are estimated to be 0.814 and 6.49 D.

For pyridine- I_2 ($\lambda_{\text{max}}^{\text{ct}} = 235 \text{ nm}$, $\epsilon_{\text{max}}^{\text{ct}} = 41400 \text{ l. mol}^{-1} \text{ cm}^{-1}$), the extinction coefficient is somewhat greater than that for $\text{CHA} \cdot \text{I}_2$; however, it has been argued¹⁸ that pyridine can function simultaneously as an n donor and a π donor in pyridine- I_2 and that the large value of $\epsilon_{\text{max}}^{\text{ct}}$ is attributable to a combination of $n \rightarrow \sigma_u$ and $\pi_z \rightarrow \sigma_u$ CT transitions. The trend of $\lambda_{\text{max}}^{\text{ct}}$ from pyridine- I_2 to $\text{CHA} \cdot \text{I}_2$ is in the direction predicted by the order of complex stability.¹⁷

Figure 1 shows the spectra of the $\text{CHA} \cdot \text{I}_2$ in CCl_4 at several temperatures. Using the known extinction coefficient of the maximum of the blue-shifted band, the concentration of complex and formation constant can be determined; K_{DA} values for the complex in CCl_4 at 15 , 25 , and 35° are evaluated to be 307, 177, and 107 l. mol^{-1} , respectively. The K_{DA} value at 25° is in good agreement with that obtained from the solubility method. The values of ΔH° , ΔG° , and ΔS° are determined to be -9.5 kcal/mol , -3.07 kcal/mol , and 20.9 eu/mol for the $1 M$, ideal dilute solution standard state in CCl_4 . Again, comparison of the thermodynamic results with those for pyridine- I_2 in CCl_4 ($\Delta H^\circ = -7.47 \text{ kcal/mol}$, $\Delta S^\circ = 15.8 \text{ eu/mol}$) indicates that $\text{CHA} \cdot \text{I}_2$ is the stronger complex. From the frequency of CT band, an ionization potential of 9.1 eV for the nonbonding electrons localized on N(1) is estimated for CHA.

Acknowledgment is made to the National Science Foundation (Grant No. GP-33519X) for support of this research.

(18) R. S. Mulliken, *J. Amer. Chem. Soc.*, **91**, 1237 (1969).

Di-*tert*-butyl Nitroxide as a Convenient Probe for Excited Singlet States. A Study of Pyrene Luminescence

James A. Green II^{1a} and Lawrence A. Singer*^{1b}

Contribution from the Department of Chemistry, University of Southern California, Los Angeles, California 90007. Received October 23, 1973

Abstract: Di-*tert*-butyl nitroxide (DTBN) quenches both the pyrene monomer and excimer emissions in benzene solution at room temperature close to the diffusion limit: monomer, $k_Q = 8.4 \times 10^9 M^{-1} \text{ sec}^{-1}$; excimer, $k_Q = 4.1 \times 10^9 M^{-1} \text{ sec}^{-1}$. From steady-state fluorescence yield measurements and directly measured monomer and excimer lifetimes, values are derived for several important parameters of the pyrene monomer-excimer system.

Recently, we reported that the stable free radical di-*tert*-butyl nitroxide (DTBN) efficiently quenches the fluorescence of a series of aromatic hydrocarbons in solution at room temperature.² The viscosity dependence and rate constants for quenching k_Q suggested that the rate of the quenching reaction is very near the diffusion limit in solvents of moderate viscosity. As part of a program to test the generality of fluorescence quenching by DTBN, and to demonstrate further its capabilities and limitations as a mechanistic probe of

photochemical and photophysical processes, we have extended our study to the pyrene monomer-excimer³⁻⁷ system.

We show that the DTBN fluorescence quenching data² can be employed to provide rate parameters for

(1) (a) National Institutes of Health Predoctoral Fellow, 1968-1970 and 1972-1973; (b) Alfred P. Sloan Fellow, 1970-1972.

(2) J. A. Green II and L. A. Singer, *J. Chem. Phys.*, **58**, 2690 (1973).

(3) J. B. Birks, D. J. Dyson, and I. H. Munro, *Proc. Roy. Soc., Ser. A*, **275**, 575 (1963).

(4) Th. Förster and K. Kasper, *Z. Elektrochemie*, **59**, 977 (1955).

(5) E. Döller and Th. Förster, *Z. Phys. Chem. (Frankfurt am Main)*, **34**, 132 (1962).

(6) C. A. Parker and C. G. Hatchard, *Trans. Faraday Soc.*, **59**, 284 (1963).

(7) T. Medinger and F. Wilkinson, *Trans. Faraday Soc.*, **62**, 1785 (1966).

some of the important photophysical processes of pyrene in benzene solution. In addition, we point out some of the pitfalls involved in using DTBN in steady state experiments for the quantitative determination of values for such parameters. Finally, the quenching of the pyrene excimer demonstrates further the scope of luminescence quenching by DTBN.

Experimental Section

Materials. Pyrene (Princeton Organic Chemicals, zone-refined grade) was used as received. Benzene was distilled through a 2-ft glass column packed with glass beads and a center cut was collected. Di-*tert*-butyl nitroxide was prepared by the method of Hoffman and coworkers.⁸

Lifetime Measurements. The pulsing nitrogen laser system used in this study has been described in detail elsewhere.^{2,9} The samples were degassed in 1-cm square precision-bore Pyrex cells. The lifetimes were determined from the negative slopes of $\log(\text{intensity})$ vs. time plots for lifetimes much longer (≥ 20 nsec) than the exciting pulse. For lifetimes comparable to the exciting pulse, the linear phase plane deconvolution technique of Demas and Adamson¹⁰ was used. At low concentration (10^{-5} M) the pyrene monomer decay was exponential over 2–3 half-lives. We estimate the uncertainty in the lifetimes as $\pm 5\%$. Temperature was ambient with variations of $\pm 2^\circ$.

Fluorescence Measurements. Samples in the cells described above were degassed at 5–10 μ of pressure by at least three freeze-pump-thaw cycles. The exciting wavelength was 345 nm and the monomer and excimer emissions were monitored at 390 and 490 nm, respectively. Measurements were made on an American Instruments Co., Inc., spectrophotometer, using a 250-W Hg-Xe lamp and an IP21 phototube. Emission intensities were measured for each of the four cell faces and averaged. The internal consistency was approximately $\pm 10\%$ for a given intensity measurement. Where necessary, a small correction for absorption by DTBN of exciting light and/or fluorescence was made by a modification of the method of Parker.¹¹

Results

The effect of added DTBN on the pyrene monomer and excimer luminescence at different pyrene concentrations in benzene solution at room temperature is shown in Table I. Typical emission spectra at an intermediate pyrene concentration are shown in Figure 1. Direct lifetime measurements on the pyrene monomer and excimer emissions were made using a 100-kW pulsing nitrogen laser (3371 Å) with a pulse duration of ca. 6 nsec. The emission from the sample cell was passed through a Bausch and Lomb 0.5-m monochromator and focused on an RCA 931 or 1P21 photomultiplier (S-4 response). The resulting signal was displayed on a Tektronix 547 (1A1 plug-in unit) or Hewlett-Packard 183 oscilloscope. The monomer and excimer decays were monitored at 390 and 490 nm, respectively. The monomer lifetime ($\tau_M = k_i^{-1}$) at 10^{-5} M was derived from plots of $\log(I_0/I)$ vs. time. The excimer lifetime ($\tau_E = k_i'^{-1}$) was also calculated in this way at high pyrene concentration (5×10^{-2} M). At this concentration the monomer emission is 100% quenched and the observed excimer decay represents the true decay. In benzene solution the monomer and excimer lifetimes determined were 335 and 44 nsec, respectively.

The excimer lifetime at 10^{-3} M pyrene was obtained by considering the monomer rise and decay as the "pumping pulse" of the observed excimer emission.

(8) A. K. Hoffman, A. M. Feldman, E. Gelblum, and W. G. Hodgson, *J. Amer. Chem. Soc.*, **86**, 639 (1964).

(9) R. E. Brown, L. A. Singer, and J. Parks, *Chem. Phys. Lett.*, **14**, 193 (1972).

(10) J. Demas and A. W. Adamson, *J. Phys. Chem.*, **75**, 2463 (1971).

(11) C. A. Parker, "Photoluminescence of Solutions," Elsevier, Amsterdam, 1968, p 220.

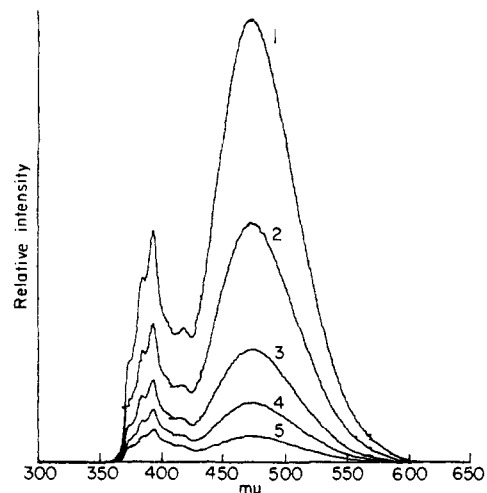


Figure 1. Emission spectra of 6×10^{-3} M pyrene in benzene solution with (1) 0 DTBN, (2) 0.8×10^{-3} M DTBN, (3) 2.4×10^{-3} M DTBN, (4) 4.0×10^{-3} M DTBN, and (5) 8.0×10^{-3} M DTBN.

Table I. Pyrene Monomer and Excimer Quenching Data

Pyrene $\times 10^3$, M	DTBN $\times 10^3$, M	$(\Phi_0/\Phi)_M^a$	$(\Phi_0/\Phi)_E^b$
0.0100	0.910	3.62	
	1.82	6.32	
	2.27	8.15	
	2.82	9.03	
1.00	0.600	1.89	1.89
	1.80	3.37	4.26
	3.00	4.77	6.95
	4.80	7.71	14.3
	8.00	12.2	27.4
3.00	0.800	1.51	1.80
	2.40	2.44	3.66
	4.00	3.48	5.62
	8.00	6.33	12.9
5.00	0.840	1.32	1.54
	4.20	2.85	5.65
	8.40	4.18	13.2
10.0	0.600	1.29	1.32
	1.80	1.35	1.93
	4.80	1.86	3.52
	8.00	2.51	5.98

^a Monitored at 3900 Å. ^b Monitored at 4900 Å.

The linear phase plane deconvolution technique¹⁰ was then used to extract the true excimer decay from the observed decays, and the excimer lifetime so obtained was 48 nsec. A similar treatment of the data obtained at 5×10^{-3} M pyrene led to a value $\tau_E = 47$ nsec.

Discussion

The fluorescence data show that DTBN quenches the monomer and excimer emissions. This result may be contrasted with the observation of Medinger and Wilkinson,⁷ who found that the heavy-atom quencher ethyl iodide was essentially ineffective as a quencher of the excimer fluorescence in ethanol. In our earlier study on fluorescence quenching by DTBN,² we concluded that the quenching mechanism by this stable free radical was either electron-exchange induced intersystem crossing,¹² $^1A^* + ^2Q \rightarrow ^3A^* + ^2Q$, or vibrational quenching,¹³ $^1A^* + ^2Q \rightarrow [^1A^*, ^2Q] \rightsquigarrow A_0 + ^2Q$, where

(12) For a discussion of this process, see G. J. Hoytink, *Accounts Chem. Res.*, **2**, 114 (1969).

(13) See A. M. Braun, W. B. Hammond, and H. G. Cassidy, *J. Amer. Chem. Soc.*, **91**, 6169 (1969).

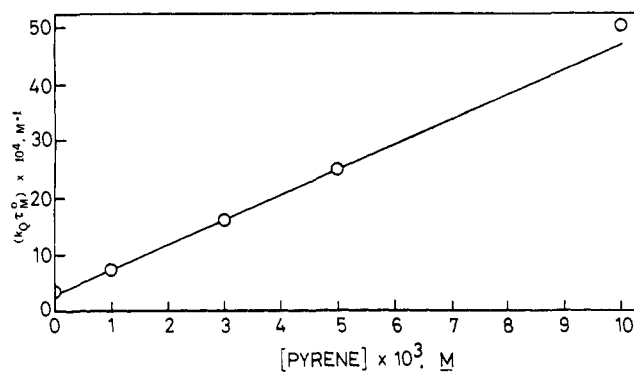
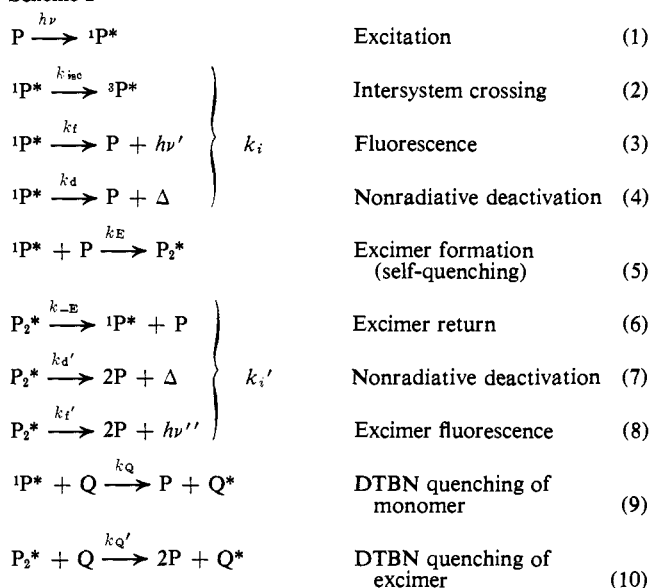


Figure 2. Dependence of the Stern-Volmer constants for monomer quenching by DTBN on the pyrene concentration.

a complex deactivates directly to ground state components with the excitation energy dissipated as vibrational energy. Our data were inconsistent with resonance-excitation exchange,¹⁴ collisional or energy-exchange transfer,¹⁵ or a charge-transfer excited state¹⁶ as the mechanism.

When the present observations are incorporated into the previously proposed mechanism for pyrene luminescence,³⁻⁷ Scheme I is obtained. For convenience in

Scheme I



calculations, steps 2-4, the unimolecular processes of the monomer, are summed as k_i , and steps 6-8, the important unimolecular excimer processes, are summed as k_i' .

Quenching of the Pyrene Monomer Emission. Steady state analysis of the reaction scheme yields the following expression for the variation of the Stern-Volmer quenching constant with variable pyrene concentration.

$$(k_Q \tau_M^0)^{-1} = k_i/k_Q + (k_E/k_Q)[P](1 - \phi_{-E}^0) \quad (I)$$

In eq I, τ_M^0 is the monomer lifetime in the absence of external quencher and $\phi_{-E}^0 = k_{-E}\tau_E^0$, which is the fraction of excimers that return to excited and ground state monomer. Figure 2 illustrates the linear relationship

(14) T. Förster, *Ann. Phys. (Leipzig)*, **2**, 55 (1948).

(15) D. L. Dexter, *J. Chem. Phys.*, **21**, 836 (1953).

(16) A. Weller, *Pure Appl. Chem.*, **16**, 115 (1968).

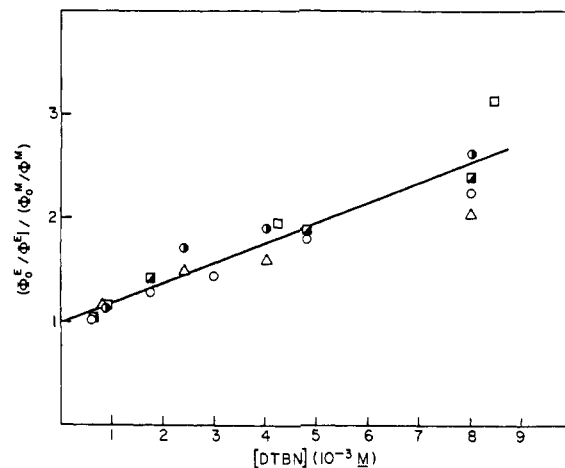


Figure 3. Plot of $(\Phi_E^E/\Phi^E)/(\Phi_M^M/\Phi^M)$ vs. DTBN concentration: (○) 10^{-3} M, (△) 3×10^{-3} M, (□) 5×10^{-3} M, (●) 6×10^{-3} M, and (◻) 10^{-2} M pyrene.

between $(k_Q \tau_M^0)^{-1}$ and $[P]$; the slope $(k_E/k_Q)(1 - \phi_{-E}^0)$, is $0.435 (\pm 10\%)$. From our earlier work,² $k_Q = 8.41 \times 10^9 M^{-1} \text{ sec}^{-1}$ in benzene, so $k_E(1 - \phi_{-E}^0) = 3.66 \times 10^9 M^{-1} \text{ sec}^{-1}$. The viscosity dependence of excimer formation⁴ and the magnitude of the rate constant reported in cyclohexane at 300°K ($k_E = 7.5 \times 10^9 M^{-1} \text{ sec}^{-1}$)³ suggest that excimer formation is very nearly diffusion controlled. If we assume that the efficiency¹⁷ of excimer formation is the same in cyclohexane and benzene, we can calculate the expected magnitude of k_E in benzene as $11.3 \times 10^9 M^{-1} \text{ sec}^{-1}$ from the relative viscosities of the two solvents (Debye equation¹⁹). Accordingly, $\phi_{-E}^0 \approx 0.67$. From this value of $\phi_{-E}^0 = k_{-E}\tau_E^0 = 0.67$, and the directly measured excimer lifetime, $k_{-E} = 1.5 \times 10^7 \text{ sec}^{-1} (\pm 15\%)$.

Quenching of the Pyrene Excimer Emission. From the kinetic scheme, the expression for quenching of the monomer emission is

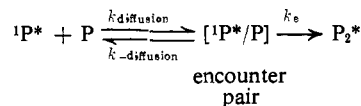
$$\Phi_M^0/\Phi_M = \{k_i + k_E[P](1 - \phi_{-E}) + k_Q[Q]\} / \{k_i + k_E[P](1 - \phi_{-E}^0)\} \quad (II)$$

where $\phi_{-E} = k_{-E}/(k_i' + k_Q'[Q])$. The expression for quenching of the excimer is

$$\Phi_E^0/\Phi_E = (1 + k_Q'\tau_E^0[Q])(\Phi_M^0/\Phi_M) \quad (III)$$

A plot of the experimentally determined values of $(\Phi_E^E/\Phi^E)/(\Phi_M^M/\Phi^M)$ (Table I) vs. DTBN concentration for the different pyrene concentrations gives a slope of $k_Q'\tau_E = 194 \pm 50 M^{-1}$ (Figure 3). From the concentration-independent excimer lifetime (~ 46 nsec), $k_Q' = 4.1 \times 10^9 M^{-1} \text{ sec}^{-1} (\pm 25\%)$. This value is somewhat

(17) Our terminology here refers to the North model for diffusion¹⁸ wherein for our system



By this model, the overall observed $k_E = k_{diff}\phi_e$, where $\phi_e = k_e/(k_e + k_{-diff})$ and is the efficiency referred to in the text.

(18) (a) A. M. North, *Quart. Rev., Chem. Soc.*, **20**, 421 (1966); (b) see also T. R. Evans, *J. Amer. Chem. Soc.*, **93**, 2081 (1971), for use of the North model in fluorescence quenching.

(19) Discussed in H. J. V. Tyrell, "Diffusion and Heat Flow in Liquids," Butterworths, London, 1961, p 127.

lower than the value k_Q obtained for monomer fluorescence quenching and may represent an inherently lower efficiency^{2,17} at the encounter pair stage for quenching of

Table II. Photophysical Parameters for the Pyrene-DTBN System in Benzene Solution at 25°

Parameter	Process	This study	Other studies
k_Q	DTBN quenching of pyrene monomer	$8.4 \times 10^9 M^{-1} \text{sec}^{-1}$	
k_Q'	DTBN quenching of pyrene excimer	$4.1 \times 10^9 M^{-1} \text{sec}^{-1}$	
k_E	Excimer formation	$11.3 \times 10^9 M^{-1} \text{sec}^{-1} \text{ }^a$	$7.5 \times 10^9 M^{-1} \text{sec}^{-1} \text{ }^b$
k_{-E}	Excimer dissociation	$1.5 \times 10^7 \text{sec}^{-1}$	$1.0 \times 10^7 \text{sec}^{-1} \text{ }^b$
τ_M	Monomer lifetime at high dilution ($10^{-5} M$)	335 nsec	435 nsec ^b
τ_E	Excimer lifetime	~46 nsec	64 nsec ^b

^a Calculated from value in cyclohexane, ref 3. ^b Reference 3, in cyclohexane.

excited state molecular aggregates by DTBN and/or a lower diffusion coefficient for the excimer relative to the

monomer.^{2,20} The present data cannot differentiate between these alternatives.

The direct lifetime measurements precluded the need for *assuming values* for bimolecular rate constants for quenching by DTBN. For example, if we had assumed in the present study that $k_Q' = k_Q = 8.4 \times 10^9 M^{-1} \text{sec}^{-1}$,² the value of τ_E^0 from the Stern-Volmer slope (eq III) would have been 23 nsec (rather than ~46 nsec), implying $k_{-E} = 2.9 \times 10^7 \text{sec}^{-1}$ (rather than $1.5 \times 10^7 \text{sec}^{-1}$) (eq I). These potential errors demonstrate that, even with a rather efficient quencher such as DTBN, great care must be exercised in assuming the magnitude of the quenching rate constants in a purely steady state experiment. Further, because of the apparently indiscriminant quenching of both singlet and triplet states²¹ by DTBN, we caution photochemists using it as a mechanistic probe to be careful in reaching conclusions about the multiplicity of reactive excited states from such data.

Acknowledgment. This work was supported by the U. S. Army Research Office, Durham.

(20) E. J. Bowen and W. S. Metcalfe, *Proc. Roy. Soc., Ser. A*, **206**, 437 (1951).

(21) R. A. Caldwell and R. E. Schwerzel, *J. Amer. Chem. Soc.*, **94**, 1035 (1972), and references therein.

Kinetics and Equilibria for Carbon Monoxide Binding to Ferrous Phthalocyanine Complexes

Dennis V. Stynes¹ and Brian R. James*²

Contribution from the Departments of Chemistry, York University, Downsview, Ontario, Canada, and University of British Columbia, Vancouver, British Columbia, Canada. Received May 26, 1973

Abstract: Six-coordinate low-spin ferrous phthalocyanine complexes ($L_2\text{FePc}$, where $L = \text{imidazole (Im)}$, pyridine (py) , piperidine (pip) , and $2\text{-methylimidazole (2-MeIm)}$) reversibly bind carbon monoxide in toluene solution *via* a dissociative mechanism. Equilibrium constants (K) for the reaction $L_2\text{FePc} + \text{CO} \rightleftharpoons \text{LFePc(CO)} + \text{L}$ decrease in the order $2\text{-MeIm} > \text{pip} > \text{py} \gg \text{Im}$. Limiting first-order rate constants for the dissociation of L parallel K . A substantial trans effect of imidazole is observed in the dissociation of CO from $L\text{FePc(CO)}$. Equilibrium and kinetic data for the phthalocyanine complexes are compared with those of some corresponding iron(II) porphyrins and glyoxime complexes, and a possible correlation between reactivity and stereochemistry of the five-coordinate intermediates is tentatively proposed.

The most important inorganic complexes in biological systems undoubtedly involve the heme group (an iron protoporphyrin IX complex). Vaska and Yamaji³ have recently reported the kinetics of the reaction of carbon monoxide with bisdiphenylglyoxime complexes of iron(II), $L_2\text{Fe(DPGH)}_2$, where $L = \text{various pyridines}$. While the reaction of these complexes with CO is qualitatively similar to the corresponding reactions of iron(II) porphyrin complexes ($L_2\text{FeP}$), kinetic and equilibrium data for the iron porphyrins show them to be far more labile and to bind CO better than the glyoxime systems;⁴ both systems involve a

dissociative mechanism and five-coordinate intermediates. The enhanced lability of ligands coordinated to axial positions of metal porphyrins has been reported for a number of normally substitution-inert metal ions.⁵⁻⁷

In order to assess those features of the porphyrin ligand which give rise to these properties, we have undertaken an investigation of the reaction of CO with another potential model for the heme group, ferrous phthalocyanine (FePc).

While FePc has long been recognized as a potential

(5) E. B. Fleischer, S. Jacobs, and L. Mestichelli, *J. Amer. Chem. Soc.*, **90**, 2527 (1968).

(6) E. B. Fleischer and M. Krishnamurthy, *J. Coord. Chem.*, **2**, 89 (1972).

(7) S. S. Eaton, G. R. Eaton, and R. H. Holm, *J. Organometal. Chem.*, **39**, 179 (1972).

(1) York University.

(2) University of British Columbia.

(3) L. Vaska and T. Yamaji, *J. Amer. Chem. Soc.*, **93**, 6673 (1971).

(4) D. V. Stynes and B. R. James, *J. Chem. Soc., Chem. Commun.*, 325 (1973).